Polymer translocation through a nanopore under a pulling force

Ilkka Huopaniemi,[1] Kaifu Luo,[1, *] Tapio Ala-Nissila,[1, 2] and See-Chen Ying[2]

[1]*Laboratory of Physics, Helsinki University of Technology,*
P.O. Box 1100, FIN-02015 HUT, Espoo, Finland
[2]*Department of Physics, Box 1843, Brown University, Providence, RI 02912-1843, U.S.A.*
(Dated: February 6, 2008)

We investigate polymer translocation through a nanopore under a pulling force using Langevin dynamics simulations. We concentrate on the influence of the chain length N and the pulling force F on the translocation time τ. The distribution of τ is symmetric and narrow for strong F. We find that $\tau \sim N^2$ and translocation velocity $v \sim N^{-1}$ for both moderate and strong F. For infinitely wide pores, three regimes are observed for τ as a function of F. With increasing F, τ is independent of F for weak F, and then $\tau \sim F^{-2+\nu^{-1}}$ for moderate F, where ν is the Flory exponent, which finally crosses over to $\tau \sim F^{-1}$ for strong force. For narrow pores, even for moderate force $\tau \sim F^{-1}$. Finally, the waiting time, for monomer s and monomer $s+1$ to exit the pore, has a maximum for s close to the end of the chain, in contrast to the case where polymer is driven by an external force within the pore.

PACS numbers: 87.15.Aa, 87.15.He

I. INTRODUCTION

The transport of biopolymers through nanopores occurs in many biological processes, such as DNA and RNA translocation across nuclear pores, protein transport through membrane channels, and virus injection [1, 2, 3]. Due to various potential technological applications, such as rapid DNA sequencing [4], gene therapy and controlled drug delivery [5], recently a number of experimental [6, 7, 8, 9, 10, 11, 12, 13, 14, 15], theoretical [15, 16, 17, 18, 19, 20, 21, 22, 23, 24, 25, 26, 27, 28, 29, 30, 31, 32, 33] and numerical [29, 30, 31, 32, 33, 34, 35, 36, 37, 38, 39, 40, 41, 42, 43] studies on polymer translocation have been carried out.

In 1996, Kasianowicz *et al.* [6] demonstrated that single-stranded DNA and RNA molecules can be driven through the α-hemolysin channel in a lipid bilayer membrane under an electric field, and the polymer length can be characterized. In addition, Li *et al.* [12] and Storm *et al.* [15] showed that a solid-state nanopore could also be used for similar experiments.

Inspired by the experiments [6, 10, 15], a number of recent theories [15, 17, 20, 27, 28, 29, 30, 31, 32, 33] have been developed for the dynamics of polymer translocation. Particularly, the scaling of the translocation time τ with the chain length N is an important measure of the underlying dynamics. Sung and Park [17] and Muthukumar [20] considered equilibrium entropy of the polymer as a function of the position of the polymer through the nanopore. Standard Kramer analysis of diffusion through this entropic barrier yields a scaling prediction of $\tau \sim N^2$ for the field free translocation. For the forced translocation, a linear dependence of τ on N was suggested, which

is in agreement with some experimental results [6, 10] for α-hemolysin channel. However, as Chuang *et al.* [29] noted, the quadratic scaling behavior for the field free translocation cannot be correct for a self-avoiding polymer. The reason is that the translocation time is shorter than the equilibration time of a self-avoiding polymer, $\tau_{equil} \sim N^{1+2\nu}$, where ν is the Flory exponent [44, 45]. According to scaling theory, they showed that for large N, translocation time scales approximately in the same manner as equilibration time. For the forced translocation, Kantor and Kardar [30] provided a lower bound for the translocation time that scales as $N^{1+\nu}$, by considering the unimpeded motion of the polymer. Most recently, we investigated both free and forced translocation using both the two-dimensional fluctuating bond model with single-segment Monte Carlo moves [32, 33] and Langevin dynamic simulations [34, 35]. For the free translocation, we numerically verified $\tau \sim N^{1+2\nu}$ by considering a polymer which is initially placed in the middle of the pore [32, 34]. For the forced translocation, we found a crossover scaling from $\tau \sim N^{2\nu}$ for relatively short polymers to $\tau \sim N^{1+\nu}$ for longer chains [33, 34]. In addition, we also found that this crossover scaling remains unaffected for heteropolymer translocation [35]. The predicted short chain exponent $2\nu \approx 1.18$ in 3D agrees reasonably well with the solid-state nanopore experiments of Storm *et al.* [15].

Polymer translocation involves a large entropic barrier, and thus most polymer translocation phenomena require a driving force, such as an external electric field used in above mentioned experiments. However, one can also envisage the use of other forces, such as a pulling force. With the development of manipulation of single molecules, polymer motion can be controlled by optical tweezers [41, 46]. This gives a motivation to study the translocation in which only the leading monomer experiences a pulling force. In addition, a new sequencing technique based on a combination of magnetic and op-

tical tweezers for controlling the DNA motion has been reported [47]. Therefore, it is of great importance to theoretically investigate the polymer translocation under a pulling force. Kantor and Kardar [30] have considered the scaling of τ with N and with the pulling force F. They have also tested the scaling behavior in a MC simulation study of the fluctuation bond model. However, as discussed below, this model is only valid for moderate pulling forces. For strong pulling forces the scaling of τ with F is different and needs to be studied carefully. To this end, in this paper we investigate polymer translocation through a nanopore under a pulling force using Langevin dynamics simulations.

II. MODEL AND METHOD

In our numerical simulations, the polymer chains are modeled as bead-spring chains. The excluded volume effects and van der Waals interactions between all pairs of beads are modeled by a repulsive LJ potential as:

$$U_{LJ}(r) = \begin{cases} 4\varepsilon \left[\left(\frac{\sigma}{r}\right)^{12} - \left(\frac{\sigma}{r}\right)^6 \right] + \varepsilon, & r \leq 2^{1/6}\sigma; \\ 0, & r > 2^{1/6}\sigma, \end{cases} \quad (1)$$

where σ is the diameter of a bead, and ε is the depth of the potential. Nearest neighbor beads on the chain is connected via a FENE spring with a potential $U_{FENE}(r) = -\frac{1}{2}kR_0^2 \ln(1 - r^2/R_0^2)$, where r is the separation between consecutive beads, k is the spring constant and R_0 is the maximum allowed separation between connected beads.

In the Langevin dynamics method, each bead is subjected to conservative, frictional, and random forces $\mathbf{F}_i^C$, $\mathbf{F}_i^F$, and $\mathbf{F}_i^R$, respectively, with [48] $m\ddot{\mathbf{r}}_i = \mathbf{F}_i^C + \mathbf{F}_i^F + \mathbf{F}_i^R$, where m is the monomer's mass. Hydrodynamic drag is included through the frictional force, which for individual monomers is $\mathbf{F}_i^F = -\xi \mathbf{v}_i$, where ξ is the friction coefficient, and $\mathbf{v}_i$ is the monomer's velocity. The Brownian motion of the monomer resulting from the random bombardment of solvent molecules is included through $\mathbf{F}_i^R$ and can be calculated using the fluctuation-dissipation theorem. The conservative force in the Langevin equation consists of several terms $\mathbf{F}_i^C = -\nabla(U_{LJ} + U_{FENE}) + \mathbf{F}_{\text{pulling}}$. The pulling force is expressed as

$$\mathbf{F}_{\text{pulling}} = F\hat{x}, \quad (2)$$

where F is the pulling force strength exerted on the first monomer and $\hat{x}$ is a unit vector in the direction perpendicular to the wall.

In the present work, we consider a 2D geometry where the wall in the y direction is described as l columns of stationary particles within distance σ from one another and they interact with the beads by the repulsive part of the Lennard-Jones potential. Wall particle positions do not change during the simulations. The pore is introduced in the wall by simply removing w beads from the wall.

III. SCALING ARGUMENTS

A. Stretching extension

Here, we first briefly recall the main results of scaling analysis pioneered by Pincus [49] who considered a polymer under traction with two forces, F and $-F$, act on its end. The elongation $L(F)$ of the chain maybe written as

$$L(F) = R\phi(\frac{R}{\zeta}), \quad (3)$$

where ϕ is a dimensionless scaling function, $R = N^\nu \sigma$, denotes the size of the unperturbed coil, and ζ is the characteristic length of the problem, $\zeta = k_B T/F$.

For weak forces, such that $F < k_B T/N^\nu \sigma$, the response is linear, i.e., $\phi(x) \sim x$, which leads to [44]

$$L(F) \sim N^{2\nu} \sigma \frac{F\sigma}{k_B T}. \quad (4)$$

For moderate forces $k_B T/N^\nu \sigma \leq F \leq k_B T/\sigma$, the chain breaks up into a one-dimensional string of blobs of size ζ. Then the elongation $L(F) \sim N$, which leads to $\phi(x) \sim x^{(1-\nu)/\nu}$. Thus, one obtains [44, 49]

$$L(F) \sim N\sigma(\frac{F\sigma}{k_B T})^{\frac{1}{\nu}-1}. \quad (5)$$

Finally for strong forces $F > k_B T/\sigma$, the chain is nearly fully extended with

$$L(F) \sim N\sigma. \quad (6)$$

In the following, we use similar arguments to analyze the extension of the tethered chain pulled with a constant force through a viscous medium. The geometrical impediment due to the finite width of the pore is neglected here. For clarity, we assume that the pulling force acts on the last monomer N. Without hydrodynamic interactions the force acting on segment n is given by

$$F_n = \xi \sum_{i=1}^{n} v_i. \quad (7)$$

where v_i is the velocity of the ith segment. At steady state when inertia can be neglected compared with the frictional force, we assume $v_i = v$ and thus

$$F_n = n\xi v. \quad (8)$$

Under this physical picture, we stress that the pulling force F equals $F_N = N\xi v$. Here, we encounter a situation in which the tension F_n is segment-dependent and where the stretching of the chain is not uniform [50, 51, 52].

To this end, we generalize Eqs. (4) and (5) to this situation, following Brochard-Wyart [50], who considered the nonuniform deformation of tethered chains in uniform solvent flow. Let $\zeta_n = k_B T/F_n$ be the n-dependent

size of the Pincus blobs and x_n the position of the nth monomer with respect to the last monomer in the direction of the pulling force. For weak forces at n, i.e., $F_n < k_B T/N^\nu \sigma$, the local elongation at site n is

$$dx_n \sim n^{2\nu-1}\sigma \frac{F_n \sigma}{k_B T}dn, \qquad (9)$$

while for moderate forces, $k_B T/N^\nu \sigma \le F_n \le k_B T/\sigma$,

$$dx_n \sim \sigma(\frac{F_n \sigma}{k_B T})^{\frac{1}{\nu}-1}dn. \qquad (10)$$

Integrating Eqs. (9) and (10) over n, one finds the deformation obeys

$$L(F) \sim N^{2\nu+1}\sigma \frac{\xi v \sigma}{k_B T} \qquad (11)$$

for weak forces and

$$L(F) \sim N^{1/\nu}\sigma(\frac{\xi v \sigma}{k_B T})^{\frac{1}{\nu}-1} \qquad (12)$$

for moderate forces. From the scaling picture, the sizes ζ_n of the Pincus blobs obey $\zeta_n \sim 1/F_n \sim 1/n \sim x^{-\nu}$. This can be compared with the case of a tethered chain subjected to a uniform solvent flow [50]. The blob size decreases in the pulling force direction, resulting in a trumpetlike shape. For strong forces, the last part of the chain in fully stretched while its free end still shows Pincus-type behavior, corresponding to the regime called stem and flower [50].

Note that Eqs.(11) and (12) can be obtained by simply replacing F in Eqs.(4) and (5) by an effective force $F_{eff} = N\xi v$, which means Eqs.(4) and (5) are still applicable when one sets $\zeta = \zeta_{eff} = k_B T/F_{eff}$.

B. Translocation time

To examine τ as a function of N under the same constant pulling force F, we need to know $L(F)$ as a function of the pulling force F, not the drag force ξv on monomer. To use Eqs. (11) and (12) we need to use relation $F = N\xi v$, which are the same as Eqs.(4) and (5) although the microscopic pictures are different.

Kantor and Kardar [30] have presented a scaling argument for the unimpeded translocation, which serves as a lower bound for the true translocation through the nanopore. The polymer travels a distance $L(F))$during the translocation process. The translocation velocity scales as F/N since the force is applied to one monomer only. Thus the translocation time should depend on N and F as $\tau \sim \frac{L(F)}{v(F)}$ [30]. For moderate forces i.e., $k_B T/N^\nu \sigma \le F_n \le k_B T/\sigma$, we have from the scaling of $L(F)$ in Eq. (12)

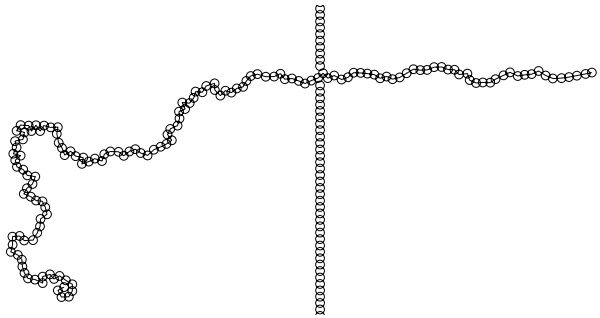$$\tau \sim \frac{L(F)}{v(F)} \sim N^2 F^{-2+\frac{1}{\nu}}. \qquad (13)$$

FIG. 1: A typical configuration of a polymer of length $N = 300$ pulled by a force of strength $F = 5$ during translocation process.

This scaling relation for moderate force is the same as the one obtained earlier [30]. We can now extend this approach to both weak and strong forces. For weak forces, the translocation time scales according to Eq.(11) as

$$\tau \sim \frac{L(F)}{v(F)} \sim N^{1+2\nu}. \qquad (14)$$

This scaling behavior is the same as that for translocation in the absence of forces [29, 32, 34], in disagreement with recent claims [53]. For strong pulling forces, the polymer becomes fully stretched and thus obtains a qualitatively different spatial configuration. Such a configuration is shown in Fig. 1 for a polymer of length $N = 300$ during translocation. In this case, the translocation time scales as

$$\tau \sim \frac{L(F)}{v(F)} \sim N^2 F^{-1}. \qquad (15)$$

Eqs. (13) and (15) show that $\tau \sim N^2$ for both moderate and strong forces. From Eqs.(14), (13) and (15), τ as a function F have three regimes with increasing F.

IV. RESULTS AND DISCUSSIONS

In our simulations, the parameters are $\sigma = 1$, $k_B T = 1.2\varepsilon$, and the time scale is given by $t_{LJ} = (m\sigma^2/\varepsilon)^{1/2}$, which is in order of ps. The friction is set as $\xi = 0.7m/t_{LJ}$. For the FENE potential, we use [54] $R_0 = 2\sigma$, $k = 7\varepsilon/\sigma^2$. Typically, $k_B T/\sigma = 4$ pN for a chain with Kuhn length $\sigma = 1$ nm at room temperature 295 K, and the time scale is about 11.28 ps for monomer mass $m = 312$ amu. The scale of the pulling force F is ε/σ, which is about 3.3 pN. The Langevin equation is integrated in time by a method described by Ermak and Buckholtz [55] in 2D. For the pore, we set $w = 3\sigma$ and $l = \sigma$ unless otherwise stated.

To create the initial configuration, the first monomer of the chain is placed in the entrance of the pore. The polymer is then let to relax to obtain an equilibrium configuration. In all of our simulations we did a number of
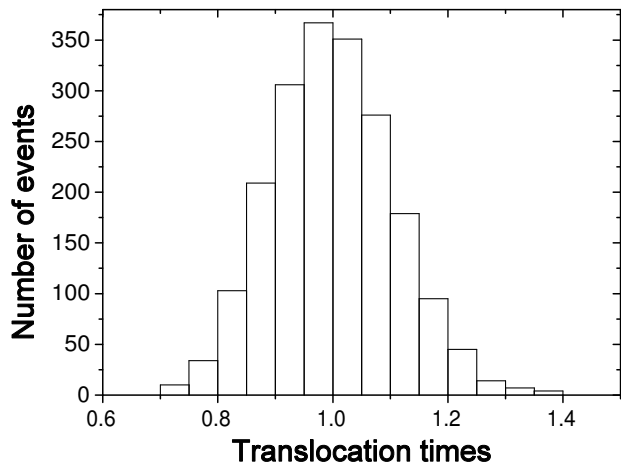
FIG. 2: The distribution of 2000 translocation times for a chain of length $N = 100$ under the pulling force of strength $F = 5$. Here, the translocation times are normalized by their average value.

runs with uncorrelated initial states. The translocation time is defined as the time interval between the entrance of the first segment into the pore and the exit of the last segment. The estimate for the translocation time was obtained by neglecting any failed translocation and then calculating the average duration of the successful translocations. Typically, we average our data over 1000 independent runs. In this section, we only investigate the translocation under the consant pulling force. For the case with the constant pulling velocity, we will examine it in detail in future.

A. Translocation time distribution

The distribution of translocation times for a polymer of length $N = 100$ pulled with a force $F = 5$ is presented in Fig. 2. The histogram obeys Gaussian distribution. This distribution has a qualitatively different shape compared to that for the free translocation case, where the corresponding distribution is asymmetric, wider and has a long tail [29, 34]. However, this distribution is quite similar to that for driven translocation under an electric field, in that it is narrow without a long tail and symmetric [30, 34]. The stronger the pulling force, the narrower the distribution becomes. As a consequence of this distribution, the average translocation time τ is well defined and scales in the same manner as the most probable translocation time. Of course, if a weak enough pulling force is used, we still can observe the long tail.

B. Waiting time

The dynamics of a single segment passing through the pore during translocation is an important issue. The non-equilibrium nature of translocation has a considerable

effect on it. We have numerically calculated the waiting times for all monomers in a chain of length N. We define the waiting time of monomer s as the average time between the events that monomer s and monomer $s + 1$ exit the pore. In our previous work [33, 34] for translocation under an electric field in the pore, we found that the waiting time depends strongly on the monomer positions in the chain. For short polymers, such as $N = 100$, the monomers in the middle of the polymer need the longest time to translocate and the distribution is close to symmetric. However, for a polymer of length $N = 300$, it's approximately the 220th monomer that needs the longest time to translocate on the other side of the pore. The waiting times for chains of length $N = 100$ and $N = 300$ under pulling forces are presented in Fig. 3. As compared to the electric field driven case [33, 34], the peaks of the waiting times are shifted towards the last monomers of the chain, independent of the force. This can be understood from the fact that when the chain is being pulled through the pore, its free energy increases due to loss of configurational entropy. For short chains, this leads to the chain motion to slow down almost monotonically until the chain entropies on both sides of the pore roughly balance each other. For long chains, the entropy of the pulled part eventually exceeds that of the remaining part of the chain and a maximum in waiting time appears close to the end of the chain.

C. Translocation time as a function of the chain length

As a reference point for comparison, we first check τ as a function of N for an infinitely wide pore, as shown in Fig. 4(a). We obtain in this case that $\tau \sim N^{1.92 \pm 0.01}$ and $\tau \sim N^{2.01 \pm 0.02}$ for $F = 5$ and 0.5 respectively. The value for $F = 0.5$ is in the moderate force regime while $F = 5$ corresponds to the strong force regime. For both these regimes, the theoretical prediction is $\tau \sim N^2$, as in Eqs. (13) and (15). Our numerical results for these two pulling forces are in very good agreement with the scaling argument predictions. For a pore of finite width, the results are shown in Fig. 4(b). We get scaling exponents of 1.87 ± 0.01 and 1.91 ± 0.02 for $F = 5$ and 0.5 respectively. These results are in excellent agreement with the Monte Carlo simulation results of Kantor and Kardar [30], and demonstrate that the scaling arguments for unimpeded translocation provides a useful estimate for the actual translocation through the finite size nanopore.

D. Translocation time as a function of the pulling force

Our theory predicts that there are three regimes in the dependence of the translocation time on the pulling force, as shown in Eqs. (14), (13) and (15). To study this, we again consider first the unimpeded translocation
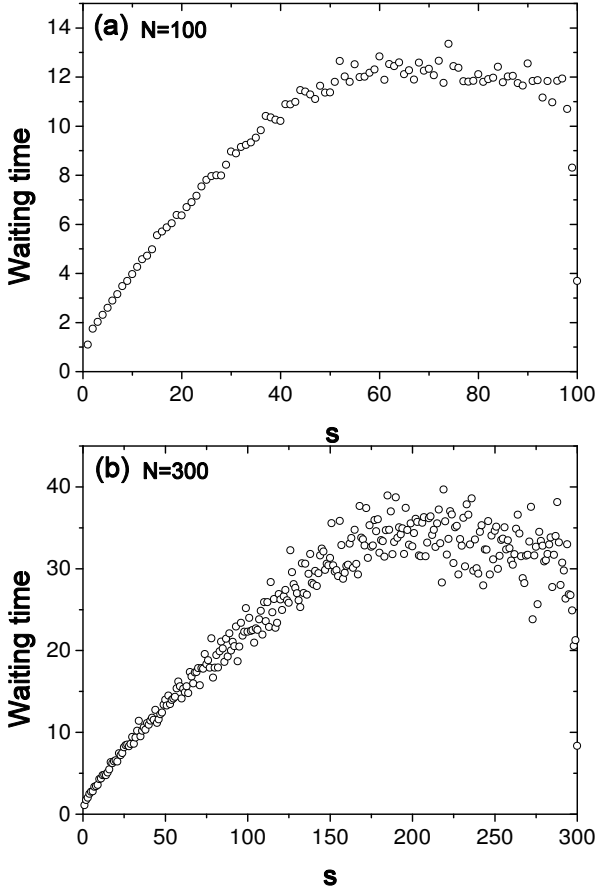
FIG. 3: Waiting times for a polymer of (a) length $N = 100$ with $F = 5$, (b) length $N = 300$ with $F = 5$.
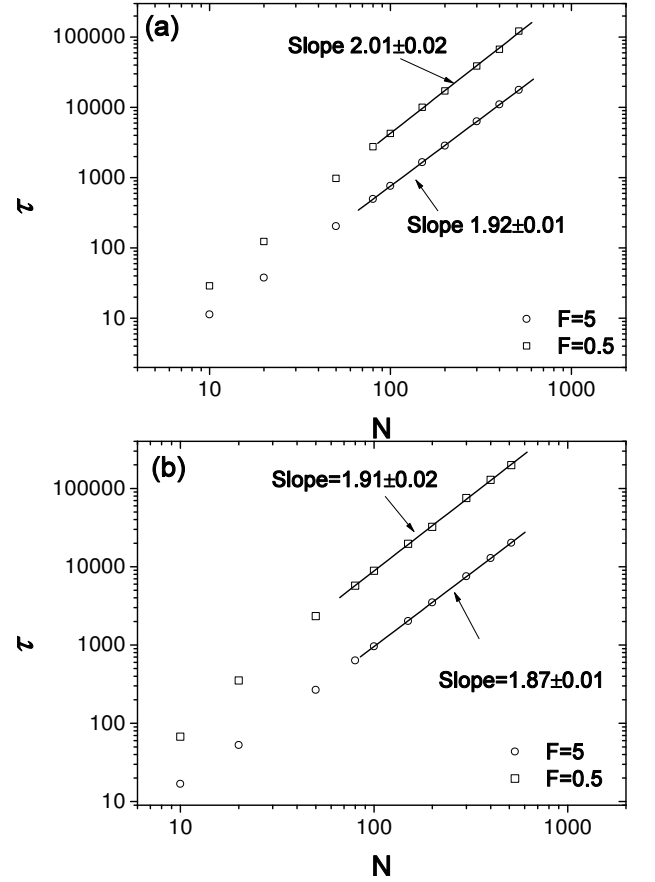

FIG. 4: The translocation time as a function of polymer length N for (a) an infinitely wide pore and (b) a pore of finite width. A constant pulling force of strength $F = 0.5$ and 5 acts on the first monomer.

through an infinitely wide pore. The numerical results in Fig. 5(a) confirm the existence of the three regimes. The translocation time is independent of F for weak pulling forces, i.e., $F \leq 0.3$, which is indicated in Eq. (14). With increasing pulling force, the translocation time scales with the force with an exponent of -0.67 for $0.3 \leq F \leq 2$. This result is in good agreement with the theoretical prediction in Eq. (13), where $\tau \sim F^{-2+\frac{1}{\nu}} \sim F^{-0.67}$ in 2D. However, for $2 \leq F \leq 10$, the exponent is -0.84. This shows that $L(F) \sim (\frac{Fa}{k_BT})^{\frac{1}{\nu}-1}$ is no longer valid since we are in the strong force regime of $F > k_BT/\sigma$. Instead, we expect $L(F)$ to be almost independent of the force and correspondingly the translocation time should scale as Eq. (15) in the limit of a strong force.

For a pore of finite width, the translocation time as a function of pulling force is presented in Fig. 5(b). For $0.25 \leq F \leq 10$ we find $\tau \sim F^{-0.94\pm0.01}$. These results show that under the restriction of the wall for a pore of finite width, it is much easier for the chain to become fully stretched and hence the strong force limit scaling behavior holds $\tau \sim F^{-1}$ through the entire range of forces applied.

Finally, it is important to note that both in the case of external field (voltage applied across the pore) [32, 33]

and pulling force driving the translocation process, there exists a fundamental difference between the Monte Carlo results for the lattice fluctuating bond model and the continum model considered here in the strong driving force limit. In the Monte Carlo study, the microscopic transition rate saturates very quickly when the external driving force increases, leading to a saturation of the velocity and the translocation time [30, 32]. This aspect of the fluctuating bond model is unrealistic and does not correspond to the true dynamics of the system. The continum model does not suffer from this artifact. As seen in Fig. 5, in the present model the translocation time τ scales as $\tau \sim F^{-1}$ up to the maximum force value studied and shows no sign of saturation. Our previous studies of the field driven translocation with both Monte Carlo and Langevin dynamics show that while the scaling behavior agree in most regimes, the same difference occurs in the strong force limit.
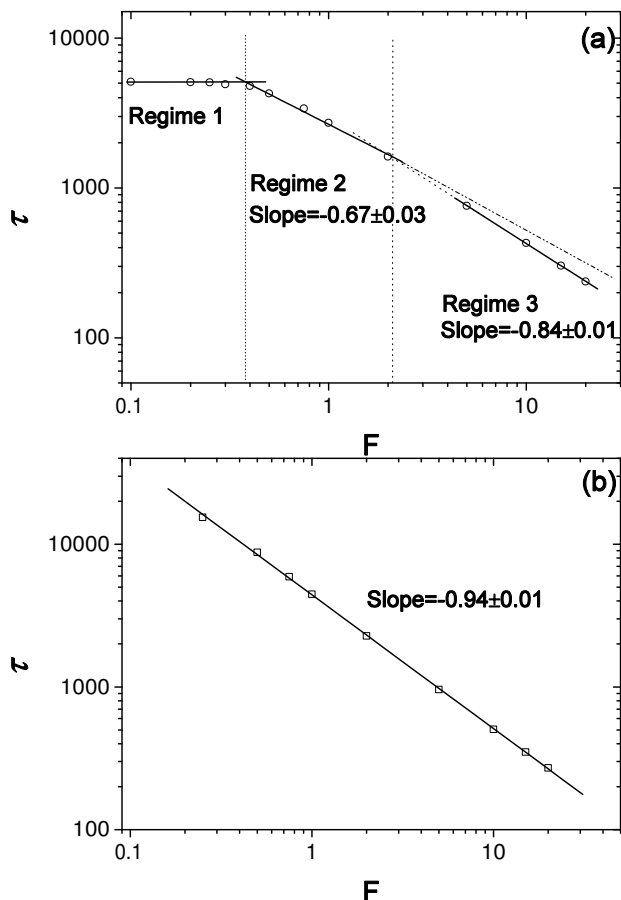
FIG. 5: Translocation time as a function of pulling force strength for (a) an infinitely wide pore and (b) a pore of finite width. τ is an average of 1000 runs. Here, $N = 100$.

V. CONCLUSIONS

In this work, we have investigated the dynamics of polymer translocation through a nanopore under a pulling force using 2D Langevin dynamics simulations. We have focused on the influence of the length of the chain N and the pulling force F on the translocation time τ. The distribution of τ is symmetric and narrow for strong F. We find that $\tau \sim N^2$ and translocation velocity $v \sim N^{-1}$ for both moderate and strong F. For infinitely wide pores, three regimes are observed for τ as a function of F. With increasing F, τ is independent of F for weak F, and then $\tau \sim F^{-2+\nu^{-1}}$ for moderate F, where ν is the Flory exponent, which finally crosses over to $\tau \sim F^{-1}$ for strong force. For narrow pores, even for moderate force $\tau \sim F^{-1}$. Finally, the waiting time, for monomer s and monomer $s + 1$ to exit the pore, has a maximum for s close to the end of the chain, in contrast to the case where polymer is driven by an external force within the pore.

Acknowledgments

[1] B. Alberts and D. Bray, *Molecular Biology of the Cell* (Garland, New York, 1994).

[2] J. Darnell, H. Lodish, and D. Baltimore, *Molecular Cell Biology* (Scientific American Books, New York, 1995).

[3] H. Salman, D. Zbaida, Y. Rabin, D. Chatenay ,and M. Elbaum, *Proc. Natl. Acad. Sci. U.S.A.* **98**, 7247 (2001).

[4] A. Meller, *J. Phys.: Condens. Matter* **15**, R581 (2003).

[5] D.-C. Chang, *Guide to Electroporation and Electrofusion* (Academic, New York, 1992).

[6] J. J. Kasianowiczs, E. Brandin, D. Branton and D. W. Deaner, *Proc. Natl. Acad. Sci. U.S.A.* **93**, 13770 (1996).

[7] M. Aktson, D. Branton, J. J. Kasianowicz, E. Brandin, and D. W. Deaner, *Biophys. J.* **77**, 3227 (1999).

[8] A. Meller, L. Nivon, E. Brandin, J. A. Golovchenko, and D. Branton, *Proc. Natl. Acad. Sci. U.S.A.* **97**, 1079 (2000).

[9] S. E. Henrickson, M. Misakian, B. Robertson, and J. J. Kasianowicz, *Phys. Rev. Lett.* **85**, 3057 (2000).

[10] A. Meller, L. Nivon, and D. Branton, *Phys. Rev. Lett.* **86**, 3435 (2001).

[11] A. F. Sauer-Budge, J. A. Nyamwanda, D. K. Lubensky, and D. Branton, Phys. Rev. Lett. **90**, 238101 (2003).

[12] J. L. Li, D. Stein, C. McMullan, D. Branton, M. J. Aziz, and J. A. Golovchenko, *Nature* (London) **412**, 166 (2001).

[13] J. L. Li, M. Gershow, D. Stein, E. Brandin, and J. A. Golovchenko, *Nat. Mater.* **2**, 611 (2003).

[14] A. J. Storm, J. H. Chen, X. S. Ling, H. W. Zandbergen, and C. Dekker, *Nat. Mater.* **2**, 537 (2003).

[15] A. J. Storm, C. Storm, J. Chen, H. Zandbergen, J. -F. Joanny and C. Dekker, *Nano Lett.* **5**, 1193 (2005).

[16] S. M. Simon, C. S. Peskin, and G. F. Oster, *Proc. Natl. Acad. Sci. U.S.A.* **89**, 3770 (1992).

[17] W. Sung and P. J. Park, *Phys. Rev. Lett.* **77**, 783 (1996).

[18] P. J. Park and W. Sung, *J. Chem. Phys.* **108**, 3013 (1998).

[19] E. A. diMarzio and A. L. Mandell, *J. Chem. Phys.* **107**, 5510 (1997).

[20] M. Muthukumar, *J. Chem. Phys.* **111**, 10371 (1999).

[21] M. Muthukumar, *J. Chem. Phys.* **118**, 5174 (2003).

[22] D. K. Lubensky and D. R. Nelson, *Biophys. J.* **77**, 1824 (1999).

[23] E. Slonkina and A. B. Kolomeisky, *J. Chem. Phys.* **118**, 7112 (2003).

[24] T. Ambjornsson, S. P. Apell, Z. Konkoli, E. A. DiMarzio, and J. J. Kasianowicz, *J. Chem. Phys.* **117**, 4063 (2002).

[25] R. Metzler and J. Klafter, *Biophys. J.* **85**, 2776 (2003).

[26] T. Ambjornsson and R. Metzler, *Phys. Biol.* **1**, 19 (2004).

[27] T. Ambjornsson, M. A. Lomholt, and R. Metzler, *J. Phys.: Condens. Matter* **17**, S3945 (2005).

[28] A. Baumgartner and J. Skolnick, *Phys. Rev. Lett.* **74**, 2142 (1995).

[29] J. Chuang, Y. Kantor and M. Kardar, *Phys. Rev. E* **65**, 011802 (2002).

[30] Y. Kantor and M. Kardar, *Phys. Rev. E* **69**, 021806 (2004).

[31] A. Milchev, K. Binder, and A. Bhattacharya, *J. Chem. Phys.* **121**, 6042 (2004).

[32] K. F. Luo, T. Ala-Nissila, and S. C. Ying, *J. Chem. Phys.* **124**, 034714 (2006).

[33] K. F. Luo, I. Huopaniemi, T. Ala-Nissila, and S. C. Ying, *J. Chem. Phys.* **124**, 114704 (2006).

[34] I. Huopaniemi, K. F. Luo, T. Ala-Nissila, and S. C. Ying, *J. Chem. Phys.* **125**, 124901 (2006).

[35] K. F. Luo, T. Ala-Nissila, S. C. Ying, and A. Bhattacharya, *J. Chem. Phys.* **126**, 145101 (2007).

[36] S.-S. Chern, A. E. Cardenas, and R. D. Coalson, *J. Chem. Phys.* **115**, 7772 (2001).

[37] H. C. Loebl, R. Randel, S. P. Goodwin, and C. C. Matthai, *Phys. Rev. E* **67**, 041913 (2003).

[38] R. Randel, H. C. Loebl, and C. C. Matthai, *Macromol. Theory Simul.* **13**, 387 (2004).

[39] Y. Lansac, P. K. Maiti, and M. A. Glaser, *Polymer* **45**, 3099 (2004).

[40] C. Y. Kong and M. Muthukumar, *Electrophoresis* **23**, 2697 (2002).

[41] Z. Farkas, I. Derenyi, and T. Vicsek, *J. Phys.: Condens. Matter* **15**, S1767 (2003).

[42] P. Tian and G. D. Smith, *J. Chem. Phys.* **119**, 11475 (2003).

[43] R. Zandi, D. Reguera, J. Rudnick, and W. M. Gelbart, *Proc. Natl. Acad. Sci. U.S.A.* **100**, 8649 (2003).

[44] P. G. de Gennes, *Scaling Concepts in Polymer Physics* (Cornell University Press, Ithaca, NY, 1979).

[45] M. Doi, and S. F. Edwards, *The Theory of Polymer Dynamics* (Clarendon, Oxford, 1986).

[46] U. Gerland, R. Bundschuh, and T. Hwa, *Phys. Biol.* **1**, 10 (2004).

[47] X. S. Lin, APS March meeting (2006).

[48] M.P. Allen, D.J. Tildesley, *Computer Simulation of Liquids* (Oxford University Press, 1987).

[49] P. Pincus *Macromolecules* **9**, 386 (1976).

[50] F. Brochard-Wyart *Europhys. Lett.* **23**, 105 (1993); **26**, 511 (1994); **30**, 387 (1995).

[51] H. Schiessel and A. Blumen *J. Chem. Phys.* **105**, 4250 (1996).

[52] T. Soddemann, H. Schiessel, and A. Blumen *J. Chem. Phys.* **57**, 2081 (1998).

[53] J. K. Wolterink, G. T. Barkema, and D. Panja, *Phys. Rev. Lett.* **96**, 208301 (2006).

[54] H. J. Limbach and C. Holm, *Computer Physics Communications* **147**, 321 (2002).

[55] D. L. Ermak and H. Buckholz *J. Comput. Phys.* **35**, 169 (1980).